

Chapter 1

Introduction

Table of contents

Conjugated and Conducting Organic Polymers: The First 150 Years	3
Background and Context	4
Materials and Devices for Organic Electronics	5
Organic Field Effect Transistors (OFETs)	5
Organic Light Emitting Diodes (OLEDs)	5
Organic Light Emitting Transistors (OLETs)	6
Organic Solar Cells (OSCs).....	6
Sensors.....	6
Properties of conjugated materials	7
Band gap.....	7
Aromatic and Quinoidal Resonance Structures.....	7
Fused Ring Systems.....	8
Donor-Acceptor (Push-Pull) Copolymers	9
Electron Withdrawing and Donating Groups	10
Electronic properties	10
Optical properties	13
Effect of Conjugation Length on the Properties of Conjugated Materials	14
Molecular weight.....	14
Torsion and planarity	15
Effect of Aggregation on the Properties of Conjugated Materials	16
π - π Stacking	16
Solvent effects.....	17
Different Conducting Polymers: Synthesis, Structure and Applications	18

Chapter 1

Aims and Objectives	24
References.....	25

Conjugated and Conducting Organic Polymers: The First 150 Years

In the twenty-first century, the majority of society has transformed into a plastic-based culture where plastics generated from organic polymers are more common place than other everyday materials like glass, metal, or ceramics.^{1,2} For this reason, some have argued that there is sufficient evidence to call the era starting in the 20th century the Age of Plastics.^{3,4} Despite the fact that plastics made from common organic polymers, like polyethylene or polystyrene, are electrically insulating, it was shown in the 1960s that certain classes of organic polymers could be made to behave semiconducting, with conductivity values that by the late 1970s rivalled those of metals.^{5,6}

Conjugated organic polymers, a family of organic semi-conducting materials that display improved electronic conductivity in their non-neutral redox states, are typically the source of conductive organic polymers (Figure 1.1).^{7,8} So, these polymers combine many of the advantageous qualities of organic plastics, such as low production costs and mechanical flexibility, with the electrical properties of traditional inorganic materials.^{9,10} A multitude of technical applications and the contemporary field of organic electronics have been developed as a result of this special blend of features, which has sparked ever-increasing fundamental and technological curiosity. Organic photovoltaics (OPVs), organic light-emitting diodes (OLEDs), field effect transistors (FETs), electrochromic devices, and a variety of sensors are examples of such applications.^{7,8,11,12}

The history of conducting polymers has been documented by a number of authors, but these accounts typically depict the field's development as relatively recent, having started in the mid-to-late 1970s with the joint work of Hideki Shirakawa, Alan G. MacDiarmid, and Alan J. Heeger on conducting polyacetylene.⁵ This widespread perception that conducting polymers were first discovered through the work of polyacetylene has been strengthened even more by the 2000 Chemistry Nobel Prize in Chemistry being given to these researchers for the discovery and development of electrically conductive polymers.¹³ This widely believed story, however, misses the fact that reports of electrically conducting polymers first appeared in the early 1960s^{8,14,15}, and that conjugated polymers like saw holes were first studied in the early 19th

century.^{16,17} Indeed, there has been a practically constant stream of articles on the synthesis and study of polyaniline spanning back over the last 180+ years, leading some to suggest that it is the earliest known entirely synthesized organic polymer and even predates polystyrene.^{10,18,19}

Background and Context

Large portion of the early history of conjugated polymers predates the introduction of the macromolecular model of polymers by Hermann Staudinger (1881–1965) in the 1920s as well as the capacity to discern the molecular structure of the materials being described.^{10,20} Moreover, the term "polymer" was first used in 1832 by Jacob Berzelius (1779–1848), just two years before the first mention of the substance now known as polyaniline, and its original meaning differed greatly from its current usage.²¹ Because of this, the early studies of conjugated polymers did not indicate the mass of polymers or macromolecules; instead, the only information that puts this work in a contemporary context is study of the chemical processes and attributes stated.²² Because of this, it is worthwhile to quickly go over the current understanding of the techniques employed in these early studies as well as the fundamental redox doping of these polymers in order to set the stage for the information that will be covered in the parts that follow.²³ The main processes used to create modern conjugated materials are direct arylation polymerization and transition metal-catalyzed cross-coupling techniques (Stille, Suzuki, Kumada, etc.)^{19,24,25} On the other hand, throughout their early history, oxidative polymerization limited the synthesis of these minerals.^{1,26,27}

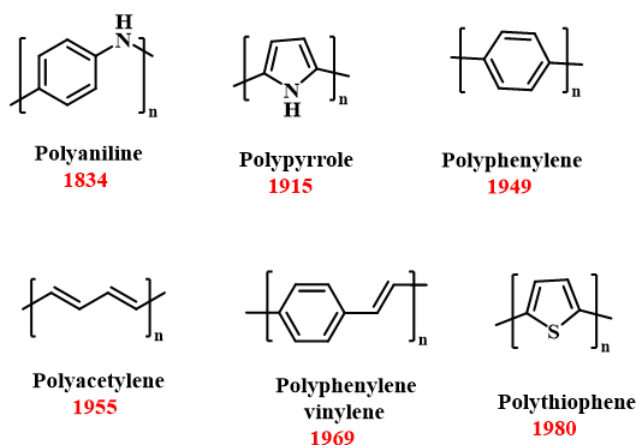


Figure 1.1 Reported conjugated polymers with the years of their first report.

Materials and Devices for Organic Electronics

Organic electronics have emerged as a promising field of research and development, drawing significant attention in recent years.²⁸ The numerous advantages associated with organic electronics contribute to their potential applications in various devices.²⁹ Organic materials used in electronic devices often exhibit high flexibility, allowing for the fabrication of flexible and bendable electronic components.³⁰ This is particularly advantageous for applications such as flexible displays, wearable electronics, and conformable sensors.³¹ Organic materials can be processed using solution-based techniques, such as printing or coating, which are more cost-effective and scalable compared to traditional semiconductor manufacturing processes.^{32,33} This ease of processing opens up opportunities for large-scale production. The use of organic materials, along with solution-based processing techniques, contributes to lower fabrication costs compared to conventional inorganic semiconductor devices. This cost-effectiveness is a significant advantage, especially for applications where cost is a critical factor.^{34,35} Organic electronics can be fabricated over large areas, making them suitable for applications that require large displays, photovoltaic panels, or sensing devices covering extensive surfaces.³⁶

The applications including organic solar cells, organic memory devices, organic thin-film transistors, organic light-emitting diodes (OLEDs), organic photodetectors and organic sensors, showcase the versatility of organic electronics.³⁷ Organic electronics is indeed a rapidly advancing interdisciplinary field that explores the unique optical and electrical properties of π -conjugated organic materials, including small molecules, oligomers, and polymers. The key motivation behind the growth of this field is the potential application of these materials in various electronic and optoelectronic devices.³⁸⁻⁴⁰

Organic Field Effect Transistors (OFETs): OFETs are a fundamental component of organic electronics. These devices utilize organic semiconductors to control the flow of charge between the source and drain electrodes, enabling the development of flexible and lightweight electronic circuits.⁴¹

Organic Light Emitting Diodes (OLEDs): OLEDs are a crucial technology in organic electronics, used for displays and lighting applications. They consist of organic compounds that emit light in response to an electric current, offering advantages such

as flexibility and improved energy efficiency compared to traditional display technologies.⁴²

Organic Light Emitting Transistors (OLETs): OLETs combine the functions of both transistors and light-emitting devices in a single structure. This integration allows for the control of light emission using electrical signals, offering potential applications in displays and other optoelectronic systems.^{42,43}

Organic Solar Cells (OSCs): Organic solar cells harness the photoactive properties of organic materials to convert sunlight into electricity. They are lightweight and flexible, making them suitable for a range of applications, including portable electronics and integration into building materials.⁴⁴

Sensors: Organic electronic materials can be employed in various sensor applications. Their unique properties make them suitable for developing sensors for detecting gases, chemicals, or biological molecules.⁴⁴

The advantages of organic electronics include their flexibility, light weight, and potential for low-cost production using solution-based processing techniques.⁴⁵ Researchers and industry professionals in this field aim to improve the efficiency, stability, and scalability of organic electronic devices to make them commercially viable for a broad range of applications. As technology continues to advance, organic electronics holds promise for shaping the future of electronic and optoelectronic devices.⁴⁶

Conjugated polymers are a specific type of organic materials characterized by a backbone structure with alternating single and double bonds between carbon atoms, forming a π -conjugated system.⁴⁷ This π -conjugation is extended through the incorporation of heteroatoms like sulphur, oxygen, or nitrogen, which contribute additional π -electrons.⁴⁸ The weak lateral overlapping between the p-orbitals in the π -conjugated system results in a smaller separation between molecular π -bonding and π -antibonding orbitals compared to σ -orbitals. This characteristic reduces the energy gap in conjugated polymers, typically falling within the range of 1.5-3.0 eV.^{31,49} Due to their semiconducting properties, conjugated polymers have gained significant attention in various applications, particularly in the fields of optoelectronics and energy-related technologies. The reduced energy gap makes them suitable for applications such as

solar cells and solar fuels production.⁵⁰ In optoelectronics, conjugated polymers are utilized for their ability to absorb light and transport charge carriers.⁴³ This makes them valuable in the development of efficient solar cells where sunlight is converted into electrical energy.⁵¹ Additionally, the semiconducting nature of these materials is exploited in energy-related applications, including the production of solar fuels. Solar fuels involve converting solar energy into chemical energy, such as through the generation of hydrogen or other fuel sources.^{52,53}

Properties of conjugated materials

Band gap

The distance between valance band and conduction band is known as band gap.⁵⁴ The band gap of any material represents the minimum energy that is require to excite the electron from valance band to conduction band.

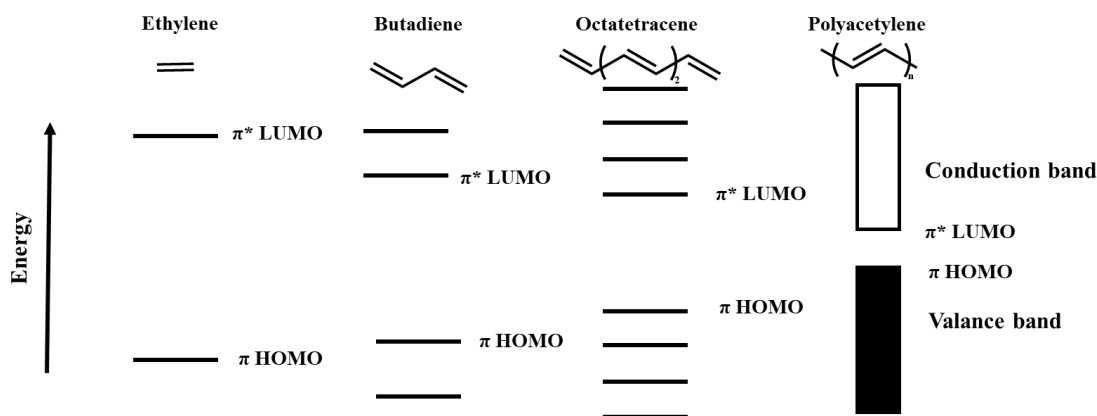


Figure 1.2 HOMO-LUMO energy level diagram with the effect of increase in conjugation.

Aromatic and Quinoidal Resonance Structures

Aromatic compounds, like benzene, exhibit a stable resonance structure where all the atoms lie in the same plane and each carbon atom contributes one π -electron to form a delocalized ring of electrons. This delocalization imparts extra stability to the molecule, making it energetically favourable. This stability is reflected in the narrower band gap of aromatic compounds compared to non-aromatic or quinoidal forms.⁵⁵

Polyphenylene serves as an example of this, since its big bandgap of around 3.2 eV is due to a strong aromaticity of benzene ring. On the other hand, the band gap (~ 2.4 eV) is lowered if double bond spacers are added between the polymeric system's phenyl

rings to create PPV. This dilutes the aromaticity. Furthermore, a quinoid form is much more likely to arise in polythiophene (which has an even lower aromaticity than benzene), as evidenced by its lower band gap energy of 2.0 eV.⁵⁶

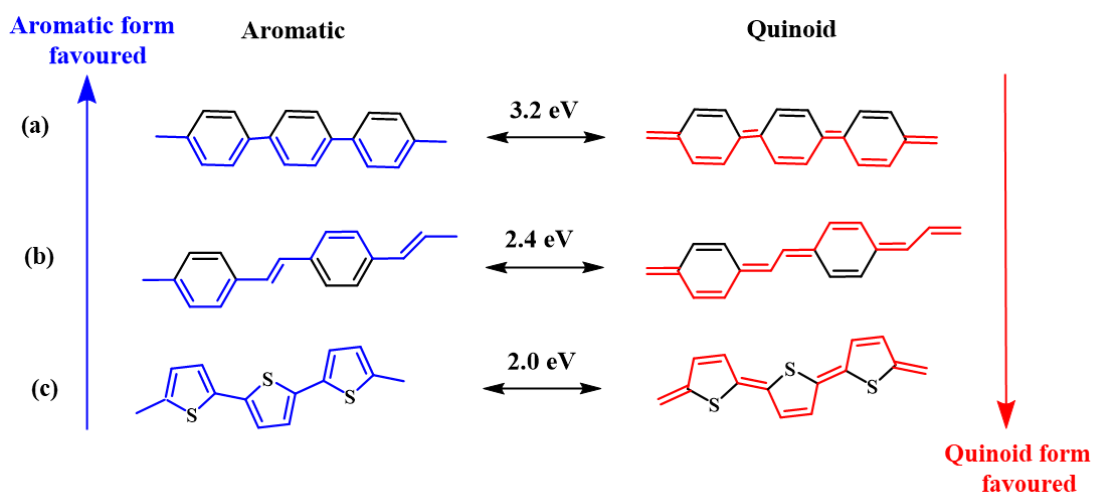


Figure 1.3 Aromatic and quinoid resonance structures of (a) polyphenylene, (b) PPV, and (c) polythiophene with their Band gap.

Fused Ring Systems

Planarizing the conjugated backbone is a second method for adjusting the bandgap. The bandgap will rise as a result of deviations from backbone planarity brought on by interring twisting and bond rotations that alter the dihedral angles between conjugated rings. More orbital overlap is produced.⁵⁷

As a result, fused ring systems that generate covalent connections between adjacent aromatic rings limit their rotation and aid in the creation of very planar conformations. Examples of effective building blocks for the synthesis of narrow bandgap polymers include fluorene, cyclopentadithiophene (CPDT), naphthobisthiadiazole (NT), and benzodithiophene (BDT), as their fused ring systems generate extremely planar structures (Figure 1.4). A polymer based on two benzothiadiazole (BT) moieties, which combined to create the naphthobisthiadiazole (NT) unit, was synthesised by Osaka *et al.*⁵⁸

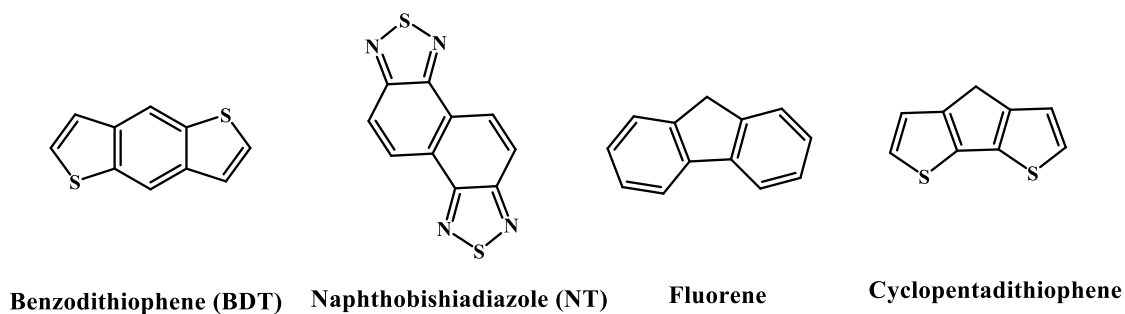


Figure 1.4 Structures of conjugated fused system.

Donor-Acceptor (Push-Pull) Copolymers

The integration of electron-rich donor (D) and electron-deficient acceptor (A) units to create alternating D-A (push pull) copolymers is the most promising bandgap engineering technique. The approach depends on the intrinsic driving force that exists between the components D and A, which promotes electron delocalization and the production of quinoid structures. In the end, however, the D and A interact to create a compressed band-gap by hybridising their molecular orbitals. The D-A copolymer has a shorter optical bandgap as a result of the interaction between the HOMO and LUMO energy levels of the D and A, which create a new, higher-lying HOMO level and a lower-lying LUMO level.

Since the bulk of the HOMO and LUMO energy levels are present in the donor and acceptor components of a D-A copolymer, respectively, it is simple to adjust the energy levels of these copolymers.⁵⁹

The amount of bandgap reduction is, however, highly dependent on the strength of the D and A units. An excessively strong acceptor, for instance, may cause the LUMO of copolymer to drop dramatically or reduce the hole mobility, which would lead to poor charge dissociation.⁶⁰

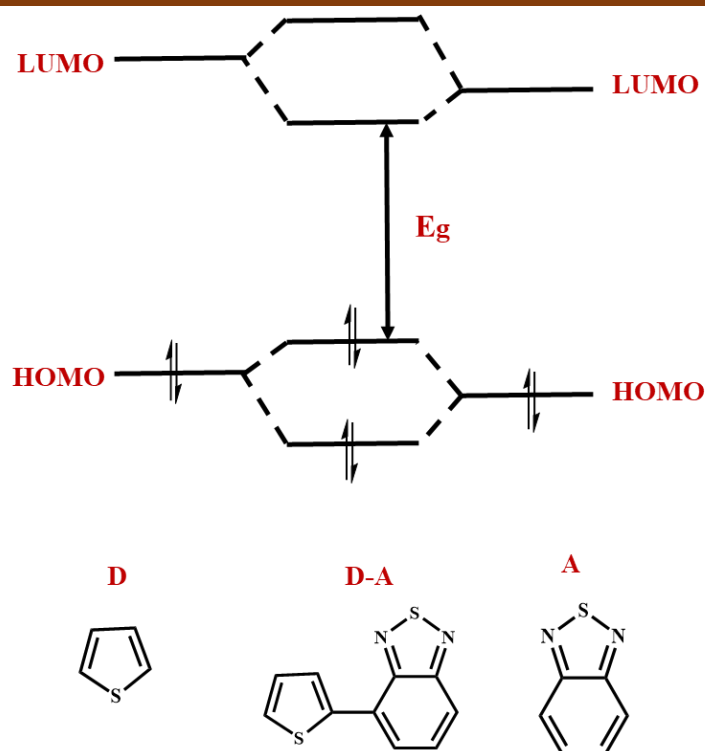


Figure 1.5 Molecular orbital hybridization diagram of donor (D) and acceptor (A) units, resulting in a narrowing of the optical band-gap in a D-A copolymer.

Electron Withdrawing and Donating Groups

Another straightforward method for creating narrow bandgap semiconductor small molecules or polymers is to attach electron-donating and/or electron-withdrawing substituents to monomer units. Bredas and Heeger (1994) investigated that how substituents affected the energy levels of poly(p-phenylene vinylene) (PPV).^{56,61} According to their study, electron-donating groups like alkoxy groups generally raise the HOMO and LUMO levels while having a greater effect on the HOMO, destabilising the frontier electronic levels, while electron-withdrawing groups like cyano groups generally lower the HOMO and LUMO levels while having a greater effect on the LUMO, stabilising the electronic levels.⁶²

Electronic properties

Conjugated materials are organic semiconductors with electronic characteristics derived from the orbitals of carbon atoms: $1s^2 2s^2 2p^2$. This allows two p orbital electrons to join together to create connections with other atoms.⁶³ Nevertheless, as Figure 1.6 illustrates, carbon atoms contain four valence electrons and can hybridise in three different ways, sp^3 , sp^2 , and sp , with $N+1$ sp^N hybridised orbitals and $3-N$ non-

hybridized p orbitals, taking into account the sp^N hybridization between atomic orbitals. Saturated polymers, including those based on alkanes, are sp^3 hybridised, show an insulating characteristic because it takes more energy than 8 eV to push an electron to the conduction band, and each carbon atom forms four σ orbitals when bound to a nearby carbon atom.⁶⁴ On the other hand, conjugated materials are based on the sp^2 hybridization of carbon atoms, which forms three coplanar bonds (σ bonds) with neighbouring atoms, each 120° apart from the other.⁶⁵ The leftover p orbital is not hybridised, remains perpendicular to the σ bonds, and overlaps with an adjacent accessible p orbital of a carbon atom to produce a double bond known as the π orbital. This overlap produces an alternating of single and double bonds in a linear chain, which is typical of conjugated polymers made of unsaturated substances like ethylene. Figure 1.7 illustrates the two divided energy levels of the π orbital: the π -bond and the π^* -anti-bond.³¹ The ethylene molecule C_2H_4 is used as an example. The π and π^* energy levels of carbon atoms degenerate in two quasi-continuous energy bands when the number of carbon atoms is high, as for real polymers like polyacetylene shown in Figure 1.7. In these bands, the bonding π -orbital represents the highest occupied molecular orbital (HOMO), and the anti-bonding π^* -orbital represents the lowest unoccupied molecular orbital (LUMO). The energy splitting, which is greater in cases where there is a greater overlap of p orbitals, is the energy required to move an electron from the ground state to an excited one ($\sim 1-3$ eV in conjugated polymers).⁶⁶ The energy splitting can be quantitatively predicted using the Linear Combination of Atomic Orbitals, LCAO.⁶⁷

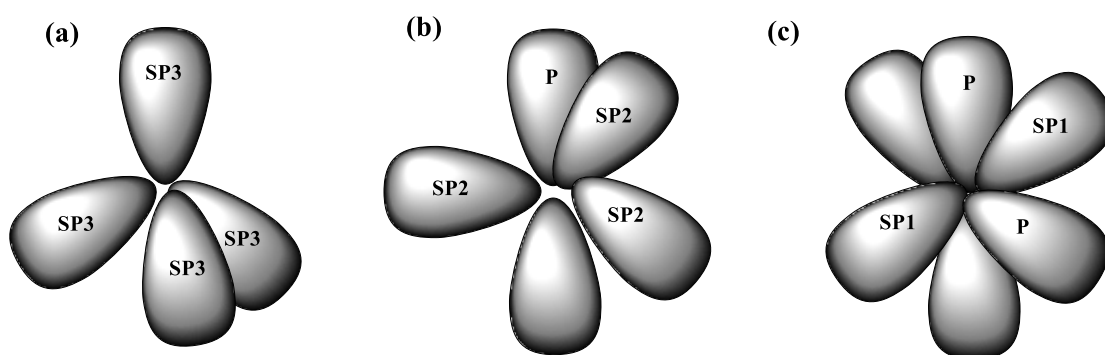


Figure 1.6 (a) sp^3 hybridization – tetrahedral structure with an angle of 109.5° . (b) sp^2 hybridization – trigonal-planar structure with an angle of 120° . (c) sp^1 hybridization – planar geometry with an angle of 180° .

Chapter 1

The HOMO-LUMO position and their energy difference, known as the Energy Gap, can be used to approximate the electronic properties of conjugated polymers, even though secondary forces like Van der Waals complicate the use of the LCAO model in solid state polymeric chains.⁶⁸

Earlier theoretical research postulated that conjugated polymers exhibited a metallic behaviour. As a result, the Energy Gap was thought to be nearly closed because of the constant distance between carbon atoms, which would cause the electron wave function to completely delocalize throughout the polymer and minimise the molecular energy.⁶⁹ The Peierls distortion, which was identified long before the electrical conductivity of doped polyacetylene was discovered in 1977, is actually responsible for the distortion for the displacement of alternating nuclei in the chain. Peierls examined how atomic oscillations disrupt the order of a periodic lattice in a one-dimensional crystal. Similar to this, if a polymeric chain is thought of as a one-dimensional crystal, the displacement of carbon nuclei decreases the symmetry of system and produces long (single) and short (double) bonds; as a result, a band separation is localised at the Brillouin zone edge.⁷⁰ It suggests that conjugated polymers have semiconducting behaviour.²¹ Hence, in Figure 1.7, a non-null and low Energy Gap ($E_g = 1.5$ eV for polyacetylene), typical of semiconductors, divides the two quasi-continuous bands of polyacetylene, HOMO and LUMO.⁷¹ There are quasi-continuous bands formed on the right as a result of the conjugation length increasing.

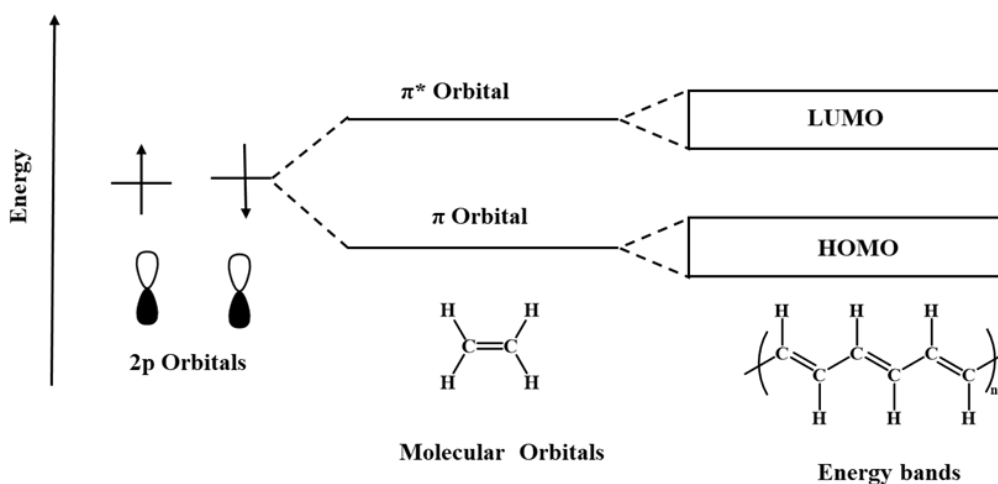


Figure 1.7 Scheme for separating two p orbitals in terms of energy into the molecular orbitals π and π^* .

Optical properties

Conjugated polymers exhibit desirable optical characteristics, including strong oscillator strengths, high photoluminescence quantum yields (near unity), tuneable Stokes' shift, and adjustable absorption and emission wavelengths from the visible ($400 \text{ nm} < \lambda_{\text{vis}} < 700 \text{ nm}$) to the near-infrared ($700 \text{ nm} < \lambda_{\text{NIR}} < 1000 \text{ nm}$) range of the spectrum.⁷² The ground state, S0, is a singlet state (i.e. total spin quantum number $S = 0$), and S1 and S2 are singlet excited states. The triplet excited state (i.e. total spin quantum number $S = 1$) is T1. Each electronic state is split in several vibrational states; whose typical energy separation is typically a fraction of meV.⁷³ Absorption is the term for the vertical transition that takes place on a fs period between the ground state and the singlet excited states.⁷⁴ By internal conversion, electrons promoted to S2 relax to the energy-lowest S1, generating no energy (no radiative processes) on the ps timescale.⁷⁵ Fluorescence is a process that occurs on a nanosecond timeline, allowing the molecule to return to its ground electron state (Kasha's rule) from the S1 level. The spin of an electron is unrestricted by Pauli's exclusion principle once it has been promoted to an excited state.⁷⁶

The surrounding environment can also affect the fluorescence properties of actual polymers, which are the features of light emission that follow photon absorption.⁷⁷ As a result, a number of things, including impurities and/or defects, such as catalyst residues or other contaminants resulting from the synthesis or contact with quenchers, might cause the fluorescence intensity to diminish. The photoluminescence yield of conjugated polymer-based devices is negatively impacted by this phenomena, which is referred to as quenching.⁷⁸ The quantum yield of photoluminescence is determined by the ratio of photons absorbed to photons released. Although quenchers always exist in solutions or liquid phases, their effectiveness is greater in solid states.⁷⁹ Indeed, the most significant source of quenching in the solid state and one that might alter the optical characteristics of conjugated polymers is molecular aggregation, also known as concentration quenching brought on by intermolecular van der Waals forces.⁸⁰ It has two distinct types of aggregates: J-aggregates (head-to-tail monomer aggregation) and H-aggregates (co-facial monomer aggregation) are the two types of monomer aggregations.⁸¹

Whereas the monomers in J-aggregates are parallel to the molecular plane, the stack of two or more monomers in H-aggregates is perpendicular to the molecular plane.⁸² In particular, absorption spectra are blue-shifted, photoluminescence quantum yield is reduced for unfavourable level splitting, and the high-energy transition is promoted in H-aggregates.⁸³ Rather, J-aggregates provide a large quantum yield and a red-shift of the optical absorption and emission, making them far more intriguing for optoelectronic and photonic applications.⁸⁴ Due to the high excitonic coupling along the J-aggregate axis, which is solely caused by Coulombic intrachain interactions, the red-shift of the optical absorption and emission of J-aggregates has been explained.⁸⁵

Effect of Conjugation Length on the Properties of Conjugated Materials

Molecular weight

The molecular weight of conjugated materials has a significant effect on their processability, optical properties, charge transporting capabilities, self-organization/crystallinity and poly dispersity, which in turn greatly influences overall device performance.⁸⁶

In addition to the previously mentioned designing of the π -extended conjugated chemical structure and suitable placement of the solubilizing alkyl chains, the molecular weight of the polymer is also crucial in obtaining highly ordered organisation of polymer chains in the solid state.⁸⁷ Polymer chain length affects morphology because tiny molecular weight polymers align face-to-face to create shorter crystalline fibres, whereas larger molecular weight polymers change the morphology of crystalline fibres into less crystalline nodular structure.⁸⁸ Furthermore, chain folding is also noted with increasing molecular weight.⁸⁹ High molecular weight polymer chains are preferred, though, as they can offer a longer channel for charge transmission. Extended polymer chains have a decreased chance of charge trapping by phase borders, which allows them to move charge more effectively in the bulk of the material even while they are unable to assemble into highly organised domains with distinct phase boundaries.⁹⁰

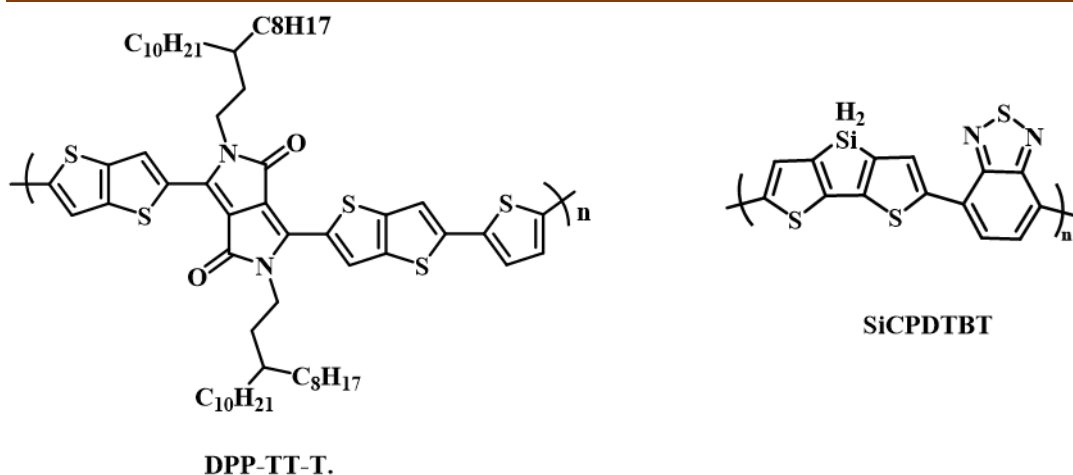


Figure 1.8 Structure of polymers reported by Vezie *et al.*⁹¹

Torsion and planarity

The effective conjugation length of a material is principally governed by planarity, and therefore any deviation from co-linearity due to twisting can have a dramatic influence on its behaviour and potential application. For OPV and OFET devices, low energy absorption and efficient charge transfer are critical, and planar layouts are favoured for two reasons: (i) They cause the bandgap to shrink by lengthening the effective conjugation length of the chain; (ii) They promote bulk intermolecular interactions between neighbouring molecules across long distances.⁹²

Vezie *et al.*⁹¹ demonstrated in the previously mentioned study that both high molecular weight and low molecular weight samples contained both *trans* (more linear) and *cis* (more curved) conformers; however, the high molecular weight samples had a higher abundance of linear conformers, which contributed to their higher overall oscillator strength/extinction coefficient. They tentatively proposed that the enhanced strength of chain-chain interactions which is maximised with a larger degree of backbone linearity, or persistence length caused high molecular weight oligomers to adopt more linear conformations.

Effect of Aggregation on the Properties of Conjugated Materials

π - π Stacking

Intramolecular charge transport refers to the movement of charges within a single molecule. Conductive polymers are a class of materials that exhibit electrical conductivity similar to metals but retain the flexibility and processability of conventional polymers. One of the key factors enabling this conductivity is their extended conjugation lengths, which result in strong π -orbital overlaps. When a polymer chain has a longer conjugation length, the delocalization of electrons along the chain becomes more efficient. This means that electrons can move more freely through the polymer structure, leading to enhanced electrical conductivity. This phenomenon is often associated with the presence of alternating single and double bonds or aromatic rings within the polymer backbone, which facilitate the formation of π -electron clouds.⁹³

In dilute solutions, polymers are typically considered as rigid rods due to the reduced intermolecular interactions between adjacent polymer chains. In this state, the polymer chains are more isolated from each other, allowing for easier intramolecular charge transport. Because there are fewer interactions between chains, the electrons within a single polymer chain can move more freely without being impeded by neighbouring chains.⁹⁴

Overall, the combination of extended conjugation lengths and reduced intermolecular interactions in dilute solutions facilitates intramolecular charge transport in conductive polymers, making them efficient materials for various electronic and optoelectronic applications. As the concentration of polymer chains increases or when they are in the solid state, the packing arrangement changes, affecting the electronic properties of the material. In these conditions, polymer chains tend to pack more closely together, promoting stronger π -conjugation between adjacent chains.⁹⁵

When the π -electron clouds of neighbouring polymer chains overlap extensively, electrons can delocalize over multiple conjugated segments, not just within a single chain but also across neighbouring chains. This phenomenon, known as intermolecular energy transfer, enables the neutral delocalization of electrons over larger distances.

As a result of this extended delocalization, inter-chain species called aggregates are formed. These aggregates have distinct electronic properties compared to isolated polymer chains. One notable effect is the red-shifted absorption and emission spectra observed in aggregates compared to individual polymer chains. This spectral shift is a consequence of the longer effective conjugation lengths and altered electronic environments within the aggregates.

The formation of aggregates and the associated changes in electronic properties play a significant role in the optoelectronic behaviour of conductive polymers in the solid state. These properties are exploited in various applications such as organic photovoltaics, light-emitting diodes, and organic semiconductor devices, where the controlled aggregation of polymer chains can be utilized to tune the optical and electronic characteristics of the material for specific purposes.

Solvent effects

The choice of solvent is a crucial factor in determining the conformation and interactions of polymer chains, as well as the extent of aggregation. Understanding these solvent-polymer interactions is essential for designing and optimizing polymer-based materials for various applications.⁸⁷

Strongly polar, non-aromatic solvents like THF block aggregation by preferentially interacting with the side groups of polymers, twisting and coiling their backbones to produce shorter average conjugation lengths. Therefore, the greater the exposure of the polymer backbones, the higher the probability of their interaction with nearby polymer chains and aggregating in solution.⁹⁶

The study by *P. Chen et al.*⁹⁷ demonstrates the significant influence of solvent choice on the morphological properties of RR-P3HT (region regular poly(3-hexylthiophene)). When cast from THF (tetrahydrofuran), the RR-P3HT chains formed defective open-coiled structures, while casting from toluene resulted in relatively regular folding to form rods.

The disparity in morphological outcomes can be attributed to the solvent quality of each solvent. Toluene, being a poor solvent compared to THF, tends to induce more pronounced chain folding and stacking behaviour in RR-P3HT. Specifically, the chains in toluene tend to coil inwards and stack with well-aligned segments. This behaviour is

driven by the desire to maximize favourable π - π interactions between adjacent segments of the polymer chains.

Overall, the study underscores the importance of solvent selection in controlling the morphological characteristics of conjugated polymer films, which in turn influences their optoelectronic properties and performance in various applications such as organic photovoltaics and field-effect transistors.

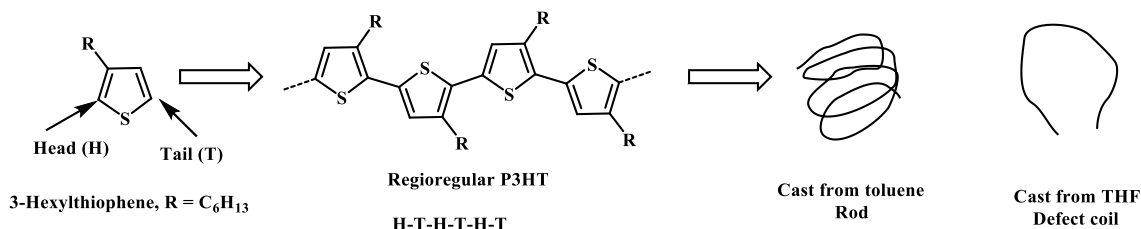


Figure 1.9 Structure of regioregular (RR) P3HT which adopts a head-to-tail (H-T) conformation and schematics of the possible conformational structures of P3HT cast from toluene and THF, namely rod and defect coil respectively.

Different Conducting Polymers: Synthesis, Structure and Applications

Solar cells based on a new acceptor-acceptor copolymer, **PF1CVTP** were described by Koetse *et al.*⁹⁸ This polymer achieves a remarkable quantum efficiency at 42%, So, as at greater light intensities that are typical for sun lighting, the conversion efficiency was dropped. **PFB** (poly (9,9-dioctylfluorene-2,7-diyl-co-bis N,N-(4-butylphenyl)-bis-N,N-phenyl-1,4-phenylenedia mine)]⁹⁹ and **F8BT** (poly(9,9-dioctylfluorene-2,7-diyl-co benzothiadiazole)¹⁰⁰ was reported by Campbell *et al* and Redecker *et al.*^{99,100} **F8BT** has a LUMO of -3.2 eV and a HOMO of -5.9 eV, while **PFB** has LUMO and HOMO energy levels are -1.9 eV and -5.1 eV, respectively. Very effective electron dissociation at the interface is apparently ensured by the comparatively significant offset of 0.8 eV for the homologous levels and 1.3 eV for the LUMO levels. The length scale on which phase separation occurs greatly relies on the solvent employed, on the interaction with the substrate, and on the conditions of deposition, according to investigations into the blend's morphology in connection to solar cell properties.

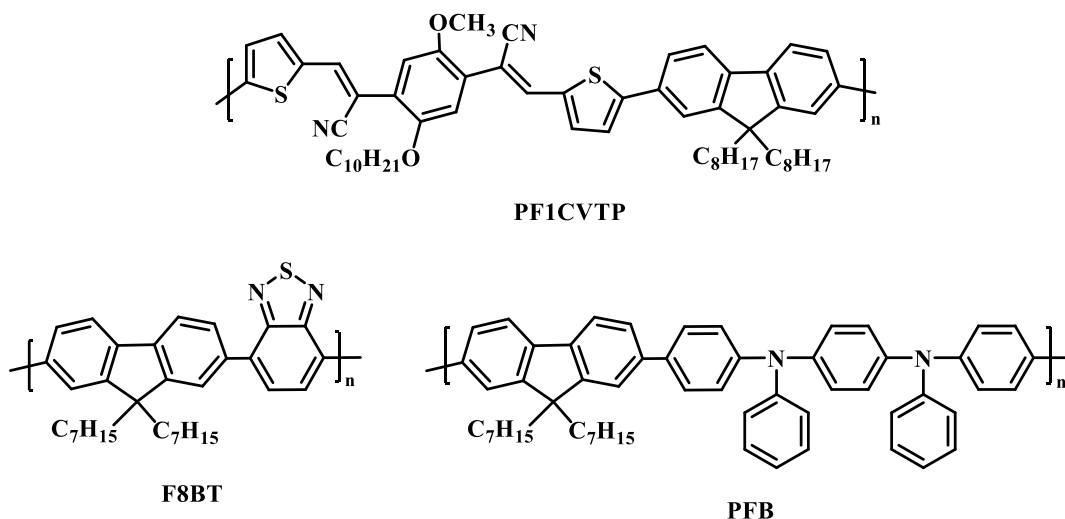


Figure 1.10 Structure of carbazole based conjugated polymers reported by Koetse *et al.*⁹⁸, Campbell *et al* and Redecker *et al.*^{99,100}

Poly(o-methoxy aniline) POMA and poly(o-ethoxyaniline) POEA was synthesized by Mattoso *et al.*¹⁰¹ Polypyrrole is basically heteroatomic conjugated polymer which are synthesised by electrochemical polymerization. Polyaniline (PAni), a conducting polymer is known for its conductivity and interesting properties, but its solubility can be limited. By introducing side groups to the polymer chain, solubility in a wider range of solvents, including water, can be achieved. However, this modification often leads to a decrease in the electrical properties compared to the parent PAni. The increase in solubility is attributed to the presence of side groups, which create more free volume within the polymer structure, reducing molecular packing and crystallization tendencies. While the electrical properties may not match those of the original PAni, they are still sufficient for many technological applications, especially when both solubility and conductivity are desired, such as in certain types of sensors, organic electronics, or biomedical applications.¹⁰²

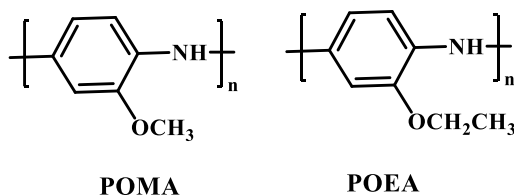


Figure 1.11 Chemical structures of poly(o-methoxyaniline) POMA and (poly(o-ethoxyaniline) POEA.

A new quinoidal acceptor building block called IQTT, which is designed to have directed diradical character to control and narrow the bandgap while maintaining good

chemical stability. Quantum mechanics simulations are used to assist in ensuring this stability. IQTT-based monomers and a donor-acceptor (D-A) polymer called PIQTT are synthesized, along with a comparison to isoindigo-based (IID) monomers and polymers (PITT). The results show that IQTT exhibits stronger electron-withdrawing ability and a more planar backbone conformation compared to IID when incorporated into copolymers. Both IQTT-based monomers and PIQTT polymers show significantly red-shifted absorption compared to their IID-based counterparts. In the solid-state, PIQTT demonstrates superior thin film order and decent field-effect transistor mobility. This work not only highlights IQTT as an excellent building block for organic electronics but also underscores the effectiveness of quantum chemical simulation tools in designing novel quinoidal narrow-bandgap D-A conjugated polymer for organic electronics.¹⁰³

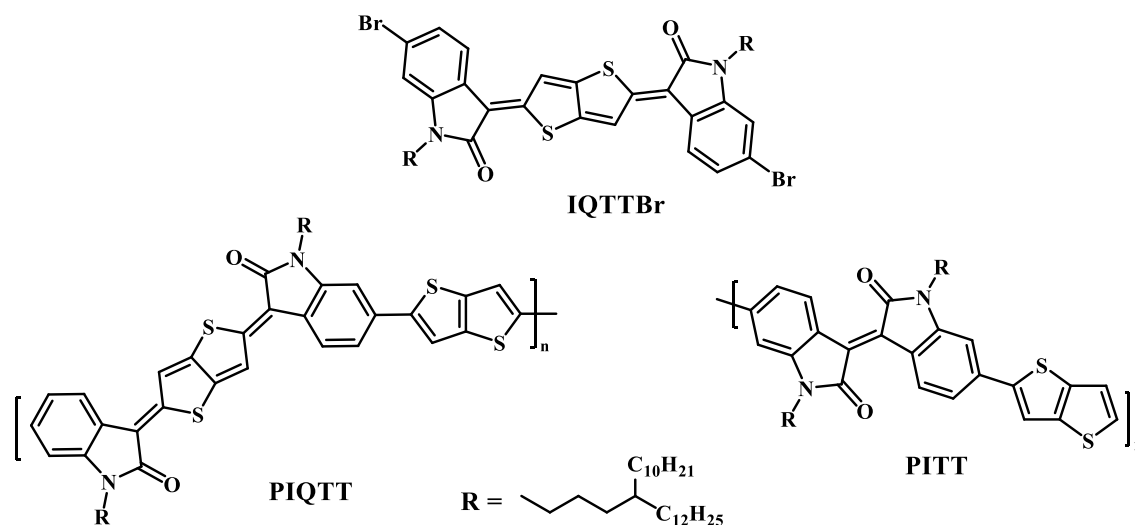


Figure 1.12 Chemical structure of diketopyrrolopyrrol based monomer conjugated polymers reported by Seng *et al.*¹⁰⁴

Seng *et al.*¹⁰⁴ reported diketopyrrolopyrrol based conjugated polymers, in this study. Poly(DPP4T-alt-TBP) having diketopyrrolopyrrole (DPP), bithiophene (BT), and biphenyl (BP) in the repeating group was successfully synthesised, despite the fact that more intricate synthetic processes were required to create the normal conjugated terpolymer. With a reasonably high current on/off ratio (>105) and a charge carrier mobility of 0.59 cm²V⁻¹s⁻¹, the Thin Film Transistor (TFT) was produced utilising a poly(DPP4T-alt-TBP) pristine film of all the devices that were produced, a PSC made of terpolymer and PC₇₁BM had the greatest power Conversion efficiency (PCE)

(4.54%), which was much higher than the PCEs of solar cells based on poly(DPP-alt-BT) and poly(DPP-alt-BP) with comparable device configurations. The short circuit current increase, which is closely linked to the internal morphology of the bulk heterojunction in mix films, is primarily responsible for the enhanced PCE of the terpolymer-based polymer solar cell (PSC). The synthesis process for this regular terpolymer offers a potential way to regulate the molecular energy levels and create a distinct crystalline shape, which can impact the performance and charge transport characteristics bulk heterojunction-type PSCs.

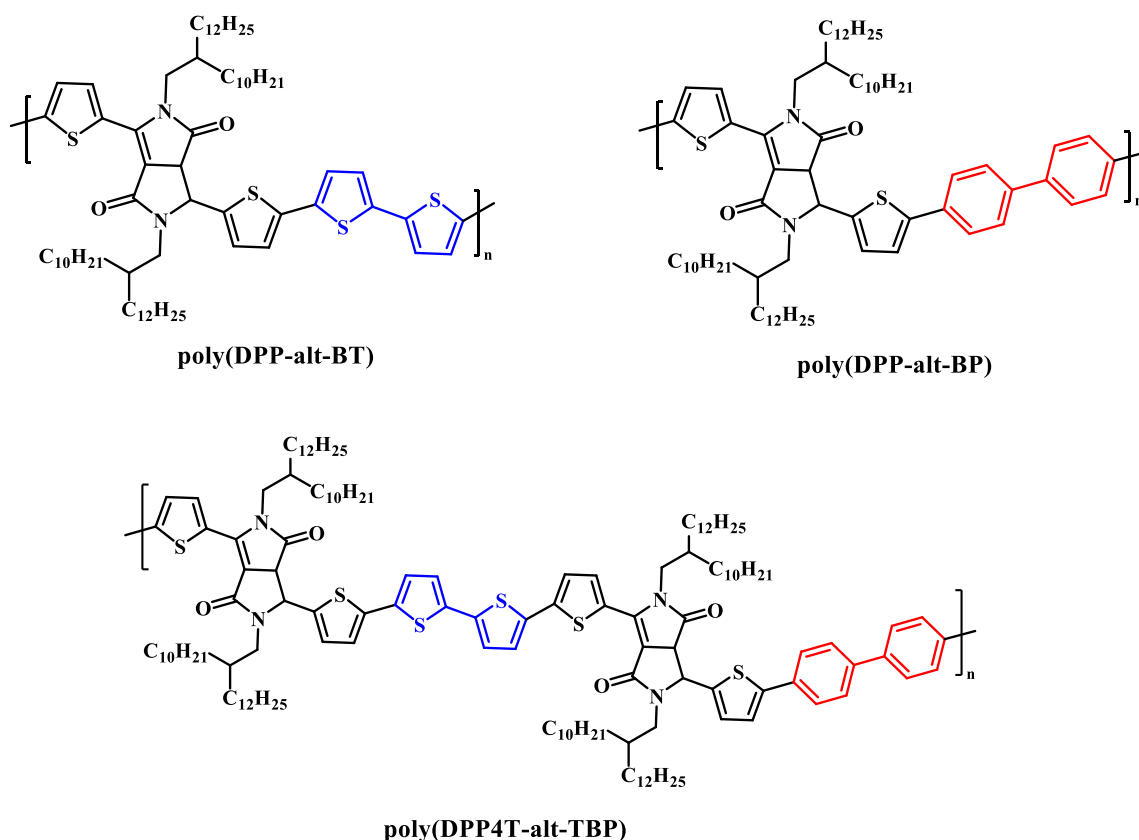


Figure 1.13 Chemical structures of diketopyrrolopyrrol based conjugated polymers.¹⁰⁴

The naphthobisthiadiazole (NT) unit was created by Osaka *et al.*¹⁰⁵ by the synthesis of a polymer based on two benzothiadiazole (BT) moieties fused together. In contrast to the BT-based polymer (1.65 eV), a reduced bandgap of 1.54 eV was possible because of its strong electron affinity and more-extended structure. It also had a high field-effect mobility (~ 0.56 cm²/Vs) and an improved PCE (6.3% compared to 2.6% for the BT-based polymer).

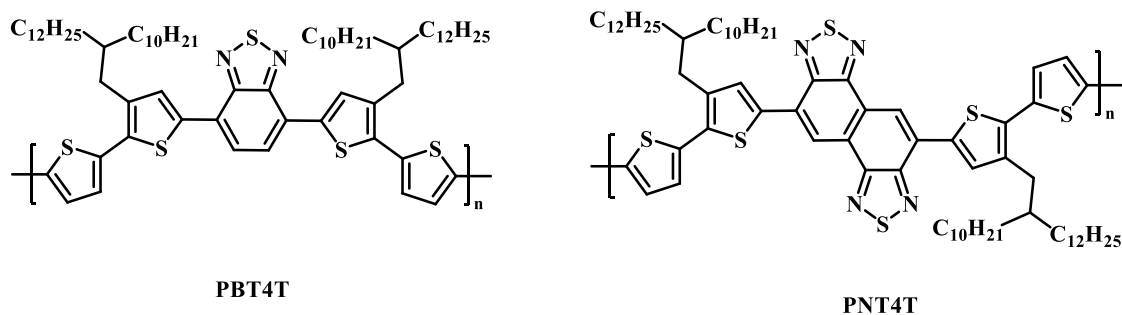


Figure 1.14 Structure of BT and NT based polymers reported by Osaka *et al.*¹⁰⁵

Polymer PTTz (Figure 1.15), the isostructural equivalent of P3HT with N atoms on alternating thiophene rings along the polymer backbone. The polymer backbone is planarized by intramolecular non-bonding N-S interactions that are created as a result of the electrically stabilising character of the N atoms in the thiazole rings. As such, lower amounts of HOMO and LUMO energy are obtained. With the fluorinated PCPDT-BT counterpart, a comparable result is seen. It was discovered that the difluoro-benzothiadiazole (DFBT) unit, which was created by adding two strong electron-withdrawing fluorine atoms to the benzothiadiazole (BT) unit, considerably improved the photovoltaic and VOC performance of the resultant polymer PCPDT-DFBT and lowered its HOMO.¹⁰⁶

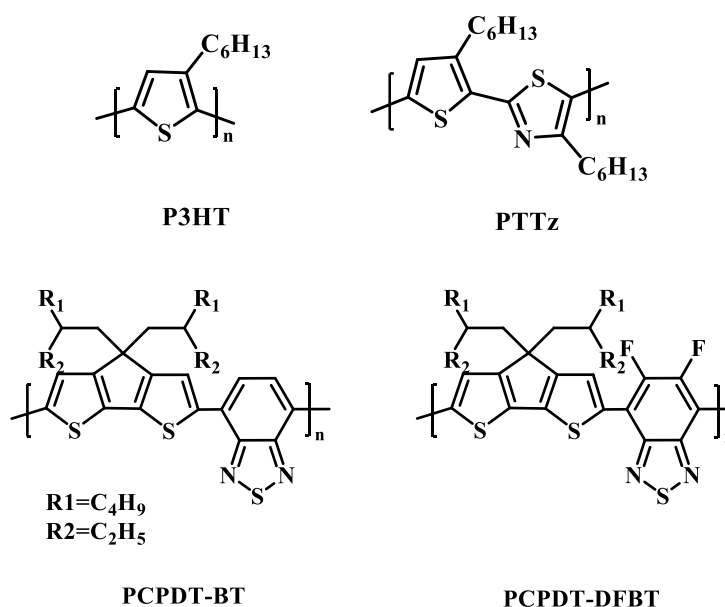


Figure 1.15 Structures of polymers P3HT vs. PTTz based on thiophene and thiophene-thiazole units respectively; and PCPDT-BT vs. PCPDT-DFBT based on benzothiadiazole and difluoro-benzothiadiazole units respectively.¹⁰⁶

Chapter 1

Primarily concentrating on the benefits of integrating aromatic fused ring structures and quinoidal structures along the polymer backbone, we have synthesized and characterized monomers with fused ring systems. Polymerization of these synthesized monomers was also carried out with different Pd-catalyst and studied them in different ways.

Aims and Objectives

- To develop a new synthetic methodology for synthesizing conjugated molecules or monomers that can be easily undergo polymerization in presence of transition metal catalyst.
- To develop conjugated polymers having a push-pull effect and having a better matched energy levels (for efficient electron/hole transfer between all layers and the electrodes of the device), that can compete favourably with other available materials for organic electronics.
- To develop conjugated small molecules having donor-acceptor concept.

References

- 1 W. Zhang, J. Smith, S. E. Watkins, R. Gysel, M. McGehee, A. Salleo, J. Kirkpatrick, S. Ashraf, T. Anthopoulos, M. Heeney and I. McCulloch, *J. Am. Chem. Soc.*, 2010, **132**, 11437–11439.
- 2 S. Günes, H. Neugebauer and N. S. Sariciftci, *Chem. Rev.*, 2007, **107**, 1324–1338.
- 3 M. C. Scharber and N. S. Sariciftci, *Prog. Polym. Sci.*, 2013, **38**, 1929–1940.
- 4 A. C. Grimsdale, K. L. Chan, R. E. Martin, P. G. Jokisz and A. B. Holmes, *Chem. Rev.*, 2009, **109**, 897–1091.
- 5 S. C. Rasmussen, 2020, *chem plus chem*, **85(7)**, 1412–1429.
- 6 C. B. Nielsen, A. Giovannitti, D. T. Sbircea, E. Bandiello, M. R. Niazi, D. A. Hanifi, M. Sessolo, A. Amassian, G. G. Malliaras, J. Rivnay and I. McCulloch, *J. Am. Chem. Soc.*, 2016, **138**, 10252–10259.
- 7 B. D. Malhotra, N. Kumar and S. Chandra, *Prog. Polym. Sci.*, 1986, **12**, 179–218.
- 8 C. K. Chiang, M. A. Druy, S. C. Gau, A. J. Heeger, E. J. Louis, A. G. MacDiarmid, Y. W. Park and H. Shirakawa, *J. Am. Chem. Soc.*, 1978, **100**, 1013–1015.
- 9 C. Kingston, M. D. Palkowitz, Y. Takahira, J. C. Vantourout, B. K. Peters, Y. Kawamata and P. S. Baran, *Acc. Chem. Res.*, 2020, **53**, 72–83.
- 10 S. C. Rasmussen, *chem comm*, 2015, **51(22)**, 4528-4543 .
- 11 Gustavo M. do Nascimento and M. A. de Souza, *Spectroscopy of Nanostructured Conducting Polymers*, 2010, **8**, 341-373.
- 12 Y. Kim, C. Park, S. Im and J. H. Kim, *Sci. Rep.*, 2020, **10**, 1–12.
- 13 H. Shirakawa, E. J. Louis, A. G. MacDiarmid, C. K. Chiang and A. J. Heeger, *J. Chem. Soc. Chem. Commun.*, 1977, 578–580.
- 14 C. K. Chiang, S. C. Gau, C. R. Fincher, Y. W. Park, A. G. MacDiarmid and A. J. Heeger, *Appl. Phys. Lett.*, 1978, **33**, 18–20.

Chapter 1

- 15 M. Ottonelli, M. Alloisio, I. Moggio, M. I. Martinez Espinosa and E. Arias, *RSC Adv.*, 2015, **5**, 83960–83968.
- 16 Seth C. Rasmussen, *Substantia*, 2017, **1**, 99–109.
- 17 B. A. Bolto and D. E. Weiss, *Aust. J. Chem.*, 1963, **16**, 1076–1089.
- 18 B. A. Bolto, R. McNeill and D. E. Weiss, *Aust. J. Chem.*, 1963, **16**, 1090–1103.
- 19 D. Feldman, *Des. Monomers Polym.*, 2008, **11**, 1–15.
- 20 Y. Li, *Organic Optoelectronic Materials*, 2015, **91**, 1-452 .
- 21 F. Babudri, G. M. Farinola and F. Naso, *J. Mater. Chem.*, 2004, **14**, 11–34.
- 22 Y. J. Cheng and T. Y. Luh, *J. Organomet. Chem.*, 2004, **689**, 4137–4148.
- 23 E. K. Solak and E. Irmak, *RSC Adv.*, 2023, **13**, 12244–12269.
- 24 P. O. Morin, T. Bura and M. Leclerc, *Mater. Horizons*, 2016, **3**, 11–20.
- 25 T. Bura, S. Beaupré, M. A. Légaré, J. Quinn, E. Rochette, J. T. Blaskovits, F. G. Fontaine, A. Pron, Y. Li and M. Leclerc, *Chem. Sci.*, 2017, **8**, 3913–3925.
- 26 R. J. Waltman and J. Bargon, *Can. J. Chem.*, 1986, **64**, 76–95.
- 27 G. D'Aprano, E. Proynov, M. Lebœuf, M. Leclerc and D. R. Salahub, *J. Am. Chem. Soc.*, 1996, **118**, 9736–9742.
- 28 G. Srivastava and R. Kumar, 2020, **110**, 2326-2341 .
- 29 P. Sarma, K. K. Sarmah, D. Kakoti, S. P. Mahanta, N. M. Adassooriya, G. Nandi, P. J. Das, D. K. Bučar and R. Thakuria, *Catal. Commun.*, 2021, **154**, 106304-106309.
- 30 A. Shukla and S. Mazumdar, *Phys. Rev. Lett.*, 1999, **83**, 3944–3947.
- 31 A. K. Mishra, *J. At. Mol. Condens. Nano Phys.*, 2018, **5**, 159–193.
- 32 A. A. D. T. Adikaari, D. M. N. M. Dissanayake and S. R. P. Silva, *IEEE J. Sel. Top. Quantum Electron.*, 2010, **16**, 1595–1606.
- 33 C. W. Lee, O. Y. Kim and J. Y. Lee, *J. Ind. Eng. Chem.*, 2014, **20**, 1198–1208.
- 34 E.-S. M. Badawy, S. E. El-Sherbeny, M. S. Hussein, H. M. F. Swaefy and H. M.

- Amer, *Med. Aromat. Plant Sci. Biotechnol.*, 2009, **3**, 9–13.
- 35 M. Reyes-Reyes, D. L. Carroll, W. Blau and R. López-Sandoval, *J. Nanotechnol.*, 2021, **12**, 1569. .
- 36 O. J. Hernández-Ortiz, D. Castro-Monter, V. Rodríguez Lugo, I. Moggio, E. Arias, M. I. Reyes-Valderrama, M. A. Veloz-Rodríguez and R. A. Vázquez-García, *Materials (Basel)*, 2023, **16**, 2908-2915.
- 37 F. Eder, H. Klauk, M. Halik, U. Zschieschang, G. Schmid and C. Dehm, *Appl. Phys. Lett.*, 2004, **84**, 2673–2675.
- 38 D. Wöhrle and D. Meissner, *Adv. Mater.*, 1991, **3**, 129–138.
- 39 H. Hoppe and N. S. Sariciftci, *J. Mater. Res.*, 2004, **19**, 1924–1945.
- 40 D. B. Mitzi, K. Chondroudis and C. R. Kagan, *IBM J. Res. Dev.*, 2001, **45**, 29–45.
- 41 H. Mohd Zahir, I. Saad, A. Roystone, A. M. Khairul, B. Ghosh and N. Bolong, *Proc. 2017 IEEE Reg. Symp. Micro Nanoelectron. RSM 2017*, 2017, 159–162.
- 42 S. Ponomarenko and S. Kirchmeyer, *Polym. Sci. Ser. C*, 2014, **56**, 1–3.
- 43 D. C. Rego, C. Sartor, N. A. Klayn and H. L. Corrêa, *J. Res. Updat. Polym. Sci.*, 2020, **9**, 24–31.
- 44 M. Ouyang, W. Q. Xiang, Y. Xu, Y. J. Zhang, Q. P. Lou and C. Zhang, *Polym. Polym. Compos.*, 2012, **20**, 21–26.
- 45 C. J. Hawker and K. L. Wooley, *Science (80-.)*, 2005, **309**, 1200–1205.
- 46 D. Moia, A. Giovannitti, A. A. Szumska, I. P. Maria, E. Rezasoltani, M. Sachs, M. Schnurr, P. R. F. Barnes, I. McCulloch and J. Nelson, *Energy Environ. Sci.*, 2019, **12**, 1349–1357.
- 47 K. Gao, L. Li, T. Lai, L. Xiao, Y. Huang, F. Huang, J. Peng, Y. Cao, F. Liu, T. P. Russell, R. A. J. Janssen and X. Peng, *J. Am. Chem. Soc.*, 2015, **137**, 7282–7285.
- 48 B. Arkles, *Organosilicon Chem. IV*, 2000, 592–612.
- 49 K. Namsheer and C. S. Rout, *RSC Adv.*, 2021, **11**, 5659–5697.
-

Chapter 1

- 50 H. Lu, X. Li and Q. Lei, *Front. Chem.*, 2021, **9**, 6–11.
- 51 W. Liu and K. P. Loh, *Acc. Chem. Res.*, 2017, **50**, 522–526.
- 52 V. Kulkarni, K. Butte and S. Rathod, *Int. J. Res. Pharm. Biomed. Sci.*, 2012, **3**, 1597–1613.
- 53 G. B. Damas, *J Phys Chem*, 2024, **128**, 2967–2977.
- 54 T. Xu and L. Yu, *Mater. Today*, 2014, **17**, 11–15.
- 55 Y. J. Cheng, S. H. Yang and C. S. Hsu, *Chem. Rev.*, 2009, **109**, 5868–5923.
- 56 C. Liu, K. Wang, X. Gong and A. J. Heeger, *Chem. Soc. Rev.*, 2016, **45**, 4825–4846.
- 57 W. R. Salaneck and J. L. Brédas, 1994, **1098**, 31–36.
- 58 I. Osaka, T. Kakara, N. Takemura, T. Koganezawa and K. Takimiya, *J. Am. Chem. Soc.*, 2013, **135**, 8834–8837.
- 59 J. T. Hou, H. S. Kim, C. Duan, M. S. Ji, S. Wang, L. Zeng, W. X. Ren and J. S. Kim, *Chem. Commun.*, 2019, **55**, 2533–2536.
- 60 B. G. Kim, X. Ma, C. Chen, Y. Ie, E. W. Coir, H. Hashemi, Y. Aso, P. F. Green, J. Kieffer and J. Kim, *Adv. Funct. Mater.*, 2013, **23**, 439–445.
- 61 J. L. Brédas, J. P. Calbert, D. A. Da Silva Filho and J. Cornil, *Proc. Natl. Acad. Sci. U. S. A.*, 2002, **99**, 5804–5809.
- 62 L. Shi, Y. Guo, W. Hu and Y. Liu, *Mater. Chem. Front.*, 2017, **1**, 2423–2456.
- 63 M. Schäferling, *Angew. Chemie - Int. Ed.*, 2012, **51**, 3532–3554.
- 64 S. Bonacchi, D. Genovese, R. Juris, M. Montalti, L. Prodi, E. Rampazzo and N. Zaccheroni, *Angew. Chemie - Int. Ed.*, 2011, **50**, 4056–4066.
- 65 F. Cicoira and C. Santato, *Adv. Funct. Mater.*, 2007, **17**, 3421–3434.
- 66 M. Demirors, *100+ Years of Plastics. Leo Baekeland and Beyond*, 2011, vol. 1080.
- 67 N. J. Hestand and F. C. Spano, *Chem. Rev.*, 2018, **118**, 7069–7163.

Chapter 1

- 68 L. Maggini and D. Bonifazi, *Chem. Soc. Rev.*, 2012, **41**, 211–241.
- 69 H. Mattoussi, G. Palui and H. Bin Na, *Adv. Drug Deliv. Rev.*, 2012, **64**, 138–166.
- 70 G. Pescitelli, L. Di Bari and N. Berova, *Chem. Soc. Rev.*, 2014, **43**, 5211–5233.
- 71 W. Y. Wong and C. L. Ho, *J. Mater. Chem.*, 2009, **19**, 4457–4482.
- 72 L. Biniek, B. C. Schroeder, J. E. Donaghey, N. Yaacobi-Gross, R. S. Ashraf, Y. W. Soon, C. B. Nielsen, J. R. Durrant, T. D. Anthopoulos and I. McCulloch, *Macromolecules*, 2013, **46**, 727–735.
- 73 M. A. Naik and S. Patil, *J. Polym. Sci. Part A Polym. Chem.*, 2013, **51**, 4241–4260.
- 74 J. H. Burroughes, D. D. C. Bradley, A. R. Brown, R. N. Marks, K. Mackay, R. H. Friend, P. L. Burns and A. B. Holmes, *Nature*, 1990, **347**, 539–541.
- 75 M. Sameiro and T. Gonçalves, *Chem. Rev.*, 2009, **109**, 190–212.
- 76 L. Basabe-Desmonts, T. J. J. Müller and M. Crego-Calama, *Chem. Soc. Rev.*, 2007, **36**, 993–1017.
- 77 C. C. Chang, M. C. Hsieh, J. C. Lin and T. C. Chang, *Biomaterials*, 2012, **33**, 897–906.
- 78 X. Feng, L. Liu, S. Wang and D. Zhu, *Chem. Soc. Rev.*, 2010, **39**, 2411–2419.
- 79 L. Jiaoli and G. Andrew C, *Chem. Soc. Rev.*, 2010, **39**, 2352–2353.
- 80 C. Zhou, Y. Liang, F. Liu, C. Sun, X. Huang, Z. Xie, F. Huang, J. Roncali, T. P. Russell and Y. Cao, *Adv. Funct. Mater.*, 2014, **24**, 7538–7547.
- 81 V. G. Kozlov and S. R. Forrest, *Curr. Opin. Solid State Mater. Sci.*, 1999, **4**, 203–208.
- 82 M. D. McGehee and A. J. Heeger, *Adv. Mater.*, 2000, **12**, 1655–1668.
- 83 M. Shimizu and T. Hiyama, *Chem. - An Asian J.*, 2010, **5**, 1516–1531.
- 84 C. W. Tang and S. A. Vanslyke, *Appl. Phys. Lett.*, 1987, **51**, 913–915.
- 85 T. Kietzke, *Adv. Optoelectron.*, 2003, **87**, 408–412. .

Chapter 1

- 86 C. Duan, F. Huang and Y. Cao, *J. Mater. Chem.*, 2012, **22**, 10416–10434.
- 87 T. Maddux, W. Li and L. Yu, *J. Am. Chem. Soc.*, 1997, **119**, 844–845.
- 88 R. J. Kline, M. D. McGehee, E. N. Kadnikova, J. Liu and J. M. J. Fréchet, *Adv. Mater.*, 2003, **15**, 1519–1522.
- 89 L. Yuan, Y. Zhao, J. Zhang, Y. Zhang, L. Zhu, K. Lu, W. Yan and Z. Wei, *Adv. Mater.*, 2015, **27**, 4229–4233.
- 90 J. F. Chang, J. Clark, N. Zhao, H. Sirringhaus, D. W. Breiby, J. W. Andreasen, M. M. Nielsen, M. Giles, M. Heeney and I. McCulloch, *Phys. Rev. B - Condens. Matter Mater. Phys.*, 2006, **74**, 1–12.
- 91 M. S. Vezie, S. Few, I. Meager, G. Pieridou, B. Dörfling, R. S. Ashraf, A. R. Goñi, H. Bronstein, I. McCulloch, S. C. Hayes, M. Campoy-Quiles and J. Nelson, *Nat. Mater.*, 2016, **15**, 746–753.
- 92 G. Conboy, H. J. Spencer, E. Angioni, A. L. Kanibolotsky, N. J. Findlay, S. J. Coles, C. Wilson, M. B. Pitak, C. Risko, V. Coropceanu, J. L. Brédas and P. J. Skabara, *Mater. Horizons*, 2016, **3**, 333–339.
- 93 B. J. Schwartz, *Annu. Rev. Phys. Chem.*, 2003, **54**, 141–172.
- 94 L. J. Fan and W. E. Jones, *Photochem. Photophysics Polym. Mater.*, 2010, 1–39.
- 95 Z. Zhou, J. Gu, X. Qiao, H. Wu, H. Fu, L. Wang, H. Li and L. Ma, *Sensors Actuators, B Chem.*, 2019, **282**, 437–442.
- 96 A. K. K. Kyaw, D. H. Wang, D. Wynands, J. Zhang, T. Q. Nguyen, G. C. Bazan and A. J. Heeger, *Nano Lett.*, 2013, **13**, 3796–3801.
- 97 Y. Kim, S. Cook, S. M. Tuladhar, S. A. Choulis, J. Nelson, J. R. Durrant, D. D. C. Bradley, M. Giles, I. McCulloch, C. S. Ha and M. Ree, *Nat. Mater.*, 2006, **5**, 197–203.
- 98 M. M. Koetse, J. Sweelssen, K. T. Hoekerd, H. F. M. Schoo, S. C. Veenstra, J. M. Kroon, X. Yang and J. Loos, *Appl. Phys. Lett.*, 2006, **88**, 88–91.
- 99 M. Redecker, D. D. C. Bradley, M. Inbasekaran, W. W. Wu and E. P. Woo, *Adv. Mater.*, 1999, **11**, 241–246.

Chapter 1

- 100 A. J. Campbell, D. D. C. Bradley and H. Antoniadis, *Appl. Phys. Lett.*, 2001, **79**, 2133–2135.
- 101 L. H. C. Mattoso, S. K. Manohar, A. G. Macdiarmid and A. J. Epstein, *J. Polym. Sci. Part A Polym. Chem.*, 1995, **33**, 1227–1234.
- 102 D. S. Correa, E. S. Medeiros, J. E. De Oliveira and L. G. Paterno, *J. Nanosci. Nanotechnol* ,2014, **14**, 1-19..
- 103 H. Jun and Y. Hu, *Macromol.* , 2019, 52, 4749-4756.
- 104 S. B. Kim, H. A. Um, H. J. Kim, M. J. Cho and D. H. Choi, *Org. Electron.*, 2016, **31**, 198–206.
- 105 I. Osaka, M. Shimawaki, H. Mori, I. Doi, E. Miyazaki, T. Koganezawa and K. Takimiya, *J. Am. Chem. Soc.*, 2012, **134**, 3498–3507.
- 106 H. Bronstein, M. Hurhangee, E. C. Fregoso, D. Beatrup, Y. W. Soon, Z. Huang, A. Hadipour, P. S. Tuladhar, S. Rossbauer, E. H. Sohn, S. Shoaee, S. D. Dimitrov, J. M. Frost, R. S. Ashraf, T. Kirchartz, S. E. Watkins, K. Song, T. Anthopoulos, J. Nelson, B. P. Rand, J. R. Durrant and I. McCulloch, *Chem. Mater.*, 2013, **25**, 4239–4249.